Viscosity of liquid sulfur under high pressure

2004 J. Phys.: Condens. Matter 16 1707

(http://iopscience.iop.org/0953-8984/16/10/003)

INSTITUTE OF PHYSICS PUBLISHING JOURNAL OF PHYSICS: CONDENSED MATTER

J. Phys.: Condens. Matter **16** (2004) 1707–1714 PII: S0953-8984(04)71494-0

Viscosity of liquid sulfur under high pressure

Hidenori Terasaki[1,6], T Kato[2], K Funakoshi[3], A Suzuki[4] and S Urakawa[5]

[1] Bayerisches Geoinstitut, Universtaet Bayreuth, 95440, Bayreuth, Germany
[2] Department of Earth and Planetary Science, Kyushu University, Fukuoka 812-8581, Japan
[3] Japan Synchrotron Radiation Research Institute, SPring-8, Hyogo 679-5198, Japan
[4] Institute of Mineralogy, Petrology and Economic Geology, Tohoku University, Sendai 980-8578, Japan
[5] Department of Earth Sciences, Okayama University, Okayama 700-8530, Japan

E-mail: Hidenori.Terasaki@Uni-Bayreuth.de

Received 6 November 2003
Published 27 February 2004
Online at stacks.iop.org/JPhysCM/16/1707 (DOI: 10.1088/0953-8984/16/10/003)

Abstract

The viscosity of liquid sulfur up to 9.7 GPa and 1067 K was measured using the *in situ* x-ray radiography falling sphere method. The viscosity coefficients were found to range from 0.11 to 0.69 Pa s, and decreased continuously with increasing pressure under approximately constant homologous temperature conditions. The observed viscosity variation suggests that a gradual structural change occurs in liquid sulfur with pressure up to 10 GPa. The L–L′ transition in liquid sulfur proposed by Brazhkin *et al* (1991 *Phys. Lett.* A **154** 413) from thermobaric measurements has not been confirmed by the present viscometry.

1. Introduction

The viscosity of liquid sulfur increases by several orders of magnitude at 432 K and ambient pressure [1, 2]. This so-called λ-transition is interpreted on the basis of structural variation in the liquid. Below the polymerization temperature ($T_p = 432$ K), liquid sulfur consists mainly of eight-membered [S_8] rings. Above 432 K, the structure of liquid sulfur changes from S_8 rings to long polymer chains [3, 4]. This polymerization corresponds to a second-order phase transition which is also accompanied by anomalous behaviour of other physical properties such as the density and heat capacity [3, 5, 6]. Therefore, structural variation in the liquid phase is closely related to changes in physical properties.

Brazhkin *et al* [7, 8] reported phase transitions in liquid sulfur at high pressure from measuring electrical resistivity and signals from thermobaric analysis. A first phase transition (L–L′) occurs in the insulator state of the liquid, with an L–L′–crystalline S triple point at $P = 7.8 \pm 0.4$ GPa and $T = 960 \pm 30$ K. A second phase transition, due to metallization, takes place near the melting point at 12 GPa (the L′–L″ transition). The L′–L″–crystalline S

[6] Author to whom any correspondence should be addressed.

triple point is located at $P = 12 \pm 0.5$ GPa and $T = 1100 \pm 30$ K. The physical properties of liquid sulfur, such as viscosity, must change at the L–L′ phase boundary if the phase transition is accompanied by structural changes.

The aim of this report is to study variation in the viscosity of liquid sulfur with pressure especially around the reported liquid–liquid phase boundary (the L–L′ transition) and investigate the possibility of observing the L–L′ transition through viscosity measurements. The viscosity of liquid sulfur was measured using the x-ray radiography falling sphere method under simultaneously high pressure and high temperature.

2. Experimental details

High pressure and temperature experiments were carried out using the multianvil press system installed at the BL04B1 beamline of the SPring-8 synchrotron facility in Japan [9]. The viscosity was measured using real time x-ray radiography to image the velocity of a sphere falling through the liquid [10]. Radiography images were collected using a high speed exposure charge coupled device (CCD) camera (C4880-80-14A, Hamamatsu Photonics KK) coupled to a YAG (yttrium aluminium garnet) fluorescence screen with a 7 μm resolution and 21–29 ms exposure time. Images were recorded on the computer hard disk with a capture rate of 30 frames per second. Calibration of the distance in the radiographic image was performed using records of the stepwise shift of the press system, which is controlled with a micrometre step. Experimental pressure was determined from the third-order Birch–Murnaghan equation of state for h-BN (hexagonal boron nitride) [11] and MgO [12], which were used as the sample capsule and x-ray window, respectively, using the following thermoelastic parameters for h-BN: $K_{T0} = 29.1 \pm 0.4$ GPa, $(\partial K_T/\partial P)_T = 9.1 \pm 0.3$ and $(\partial K_T/\partial T)_V = -0.0065 \pm 0.009$ GPa K^{-1} [11], and data for the thermal expansivity of h-BN at atmospheric pressure [13]. X-ray diffraction spectra for h-BN and MgO were collected using a Ge solid state detector (CANBERRA Inc.) at a fixed diffraction angle (2θ) of 5.5°.

The cell assembly used is shown in figure 1. The starting material was sulfur powder which was ground from sulfur crystals (99.99% in purity). Pt spheres with diameters ranging from 93 to 122 μm were used as viscosity markers, and were loaded directly into the upper part of the sample. The diameters of the spheres, listed in table 1, were measured by using scanning electron microscope imaging prior to loading in the sample. Only spheres with smooth surfaces and with the highest sphericity were used as viscosity markers. The sample container was made of h-BN which was deoxidized in advance with an induction heater at 2273 K with an N_2 flow. The initial sample size was 1.5 mm diameter and 2.0 mm height. The heater was made of cylindrical graphite and the electrodes were composed of a molybdenum foil and rod. Temperature was monitored using a W97%Re3%–W75%Re25% thermocouple, with the junction positioned just above the h-BN capsule inside the heater. No correction was made for the effect of pressure on the electromotive force. The truncated edge length of the anvils was 8 mm. The experimental conditions are listed in table 1 and the conditions plotted in figure 2 with the melting curve of sulfur from Tonkov [14]. The phase boundaries of the liquid phase, from [7, 8], are also illustrated in figure 2.

3. Results and discussion

Settling velocities of the marker spheres in the liquid sulfur were obtained from the radiographic images. Example continuous radiographic images of a falling sphere are shown in figure 3, and a falling profile obtained from these images is shown in figure 4. During the initial stages

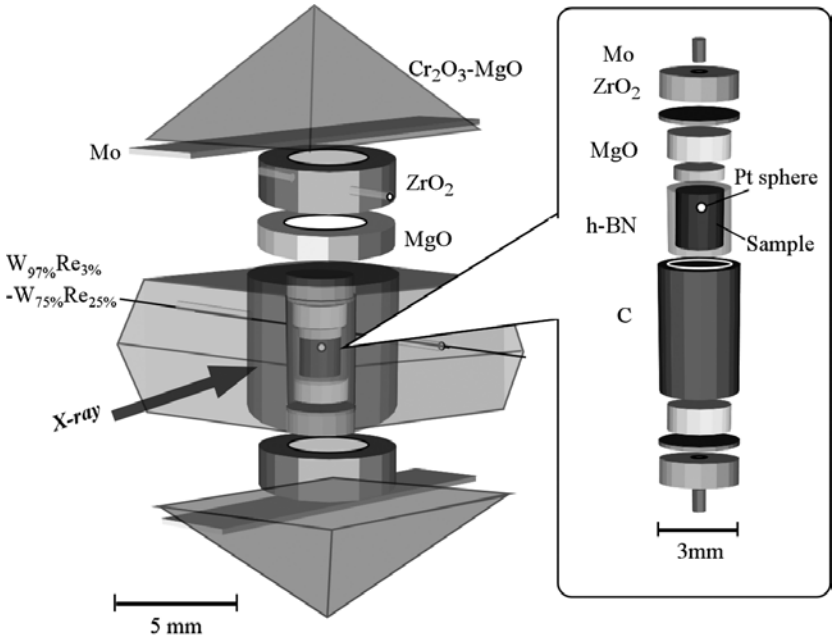

Figure 1. A schematic diagram of the cell assemblage for the viscosity measurements. The octahedral edge length of the assembly is 14 mm.

Table 1. Experimental conditions and results for liquid S.

Run No	P (GPa)	T[a] (K)	Sphere diameter (μm)	v (mm s^{-1})	η (Pa s)
S560-1	3.2(3)	788(22)	93	0.14	0.45(2)
S560-2	3.2(3)	793(11)	112	0.12	0.69(8)
S564	5.14(7)	866(10)	122	0.27	0.36(4)
S562	7.8(3)	962(8)	118	0.45	0.19(2)
S660	9.1(2)	991(6)	101	0.45	0.147(6)
S652	9.7(5)	1067(1)	94	0.53	0.105(4)

[a] The temperature error represents a change of temperature during the falling of the sphere.

of falling, we observed irregular movement of the sphere, shown by open symbols in figure 4, due to the sphere falling through partially molten material. Smooth linear points after this irregular movement, shown by closed circles in figure 4, represent sphere movement through completely molten sample. Therefore, we only used these points to determine the settling velocity. The maximum temperature difference between the cold centre and hot ends of the cell was estimated to be about 30 K, based on data from a previous study of the Fe–FeS system in which the same cell assembly was used [15]. The viscosity coefficients were calculated using Stokes' equation with wall and end correction [16, 17] as described below:

$$\eta = \frac{2gr_s^2(\rho_s - \rho_m)W}{9vE} \tag{1}$$

$$W = 1 - 2.104\left(\frac{r_s}{r_c}\right) + 2.09\left(\frac{r_s}{r_c}\right)^3 - 0.95\left(\frac{r_s}{r_c}\right)^5 \tag{2}$$

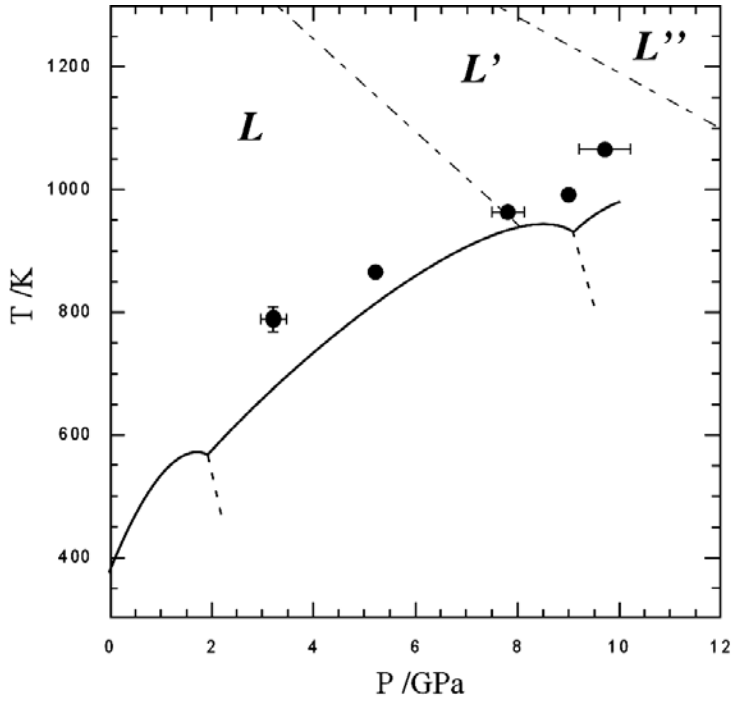

Figure 2. Experimental conditions and the melting curve of sulfur. Closed circles and the solid curve show the experimental conditions of this study and the melting curve of sulfur from [14], respectively. For reference, liquid–liquid phase boundaries from [7, 8] are also plotted as dot–dashed lines. L, L′ and L″ denote the liquid phases.

$$E = 1 + 3.3\left(\frac{r_s}{h_c}\right) \tag{3}$$

where v is the falling velocity, g is the acceleration due to gravity, ρ_s and ρ_m are the densities of the sphere and sample melt, respectively, r_s and r_c are the radius of the sphere and capsule, respectively, and h_c is the capsule height, taken to be the falling distance. The correction factors for the wall effect (W) and the end effect (E) are 0.81–0.85 and 1.21–1.30, respectively. From radiographic observation, the sphere sizes were observed to be the same before and after the settling. Therefore, the reaction between the sample and sphere is negligible during falling. The density of the platinum spheres was calculated using a Mie–Grüneisen equation of state with the compressibility data of Jamieson *et al* [12]. The third-order Birch–Murnaghan equation of state was applied for liquid sulfur. The density of liquid sulfur under the experimental conditions was calculated from the density at ambient pressure [5] with the compressibility data of Tsuchiya [18]. Since data for the pressure derivative of the bulk modulus ($\mathrm{d}K/\mathrm{d}P$) of liquid sulfur are not available, we assumed $\mathrm{d}K/\mathrm{d}P = 6 \pm 1$, which corresponds to the data of Luo and Ruoff [19] for solid phases ($\mathrm{d}K/\mathrm{d}P = 7.0$ at $P < 5$ GPa and $\mathrm{d}K/\mathrm{d}P = 5.0$ at $P > 5$ GPa). Even assuming these large uncertainties, the calculated viscosity is within 1.4%.

The measured viscosity of liquid sulfur, listed in table 1, ranges over 0.11–0.69 Pa s at the pressure and temperature conditions of 3.2–9.7 GPa and 788–1067 K. The effect of pressure on viscosity is plotted in figure 5 with the results of Ruiz-Garcia *et al* [2] measured at ambient pressure. The viscosity coefficients of Ruiz-Garcia *et al* [2] at 392 K and at 436 K are representative values for molecular liquid (S_8 rings) and for polymerized liquid,

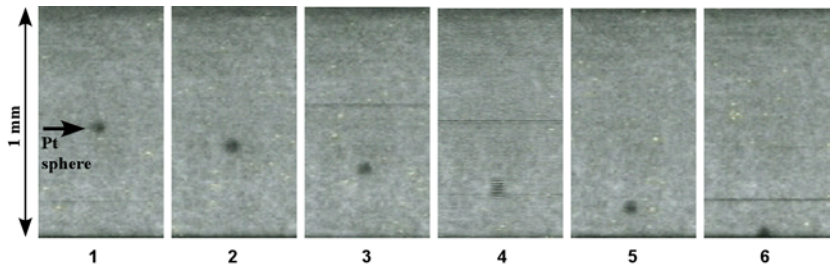

Figure 3. Continuous x-ray radiographic images of a falling sphere (run No: S652). Pt marker spheres with a diameter of 94 μm can be seen as shadows due to the high density. The time interval of each image is 0.2 s.

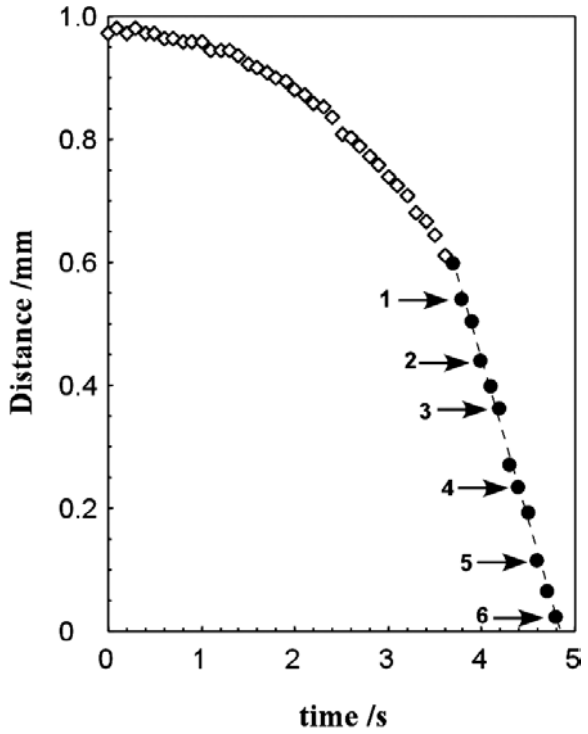

Figure 4. The time–falling distance profile of the sphere at 1067 K (run No: S652). Data used for determining the settling velocity are shown by closed circles. The width of the anvil gap corresponds to the full scale of the distance. The points shown by arrows correspond to the images shown in figure 3.

respectively. Uncertainties in measured viscosity coefficients arise from the off-centred position of the sphere in the capsule (which is related to the wall correction, $\Delta\eta = 1.1$–10.5%), the measurement error of the falling distance and capsule diameter ($\Delta\eta = 0.1$–2.0%), and the error of the sample density ($\Delta\eta = 0.6$–1.4%). Since the last two uncertainties are quite minor contributions, most of the error originates from the off-centred positioning of the sphere. We estimated total viscosity errors of 2.4%–12.0%, as listed in table 1. Although each temperature condition in figure 5 is different, the homologous temperatures, i.e. the ratios

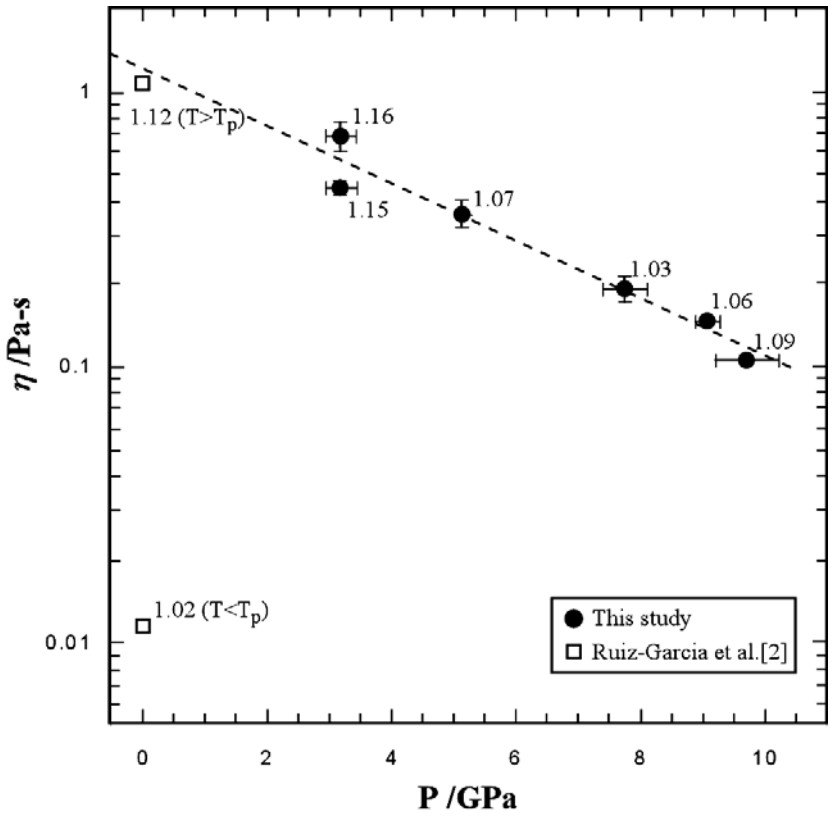

Figure 5. The pressure dependence on viscosity of liquid sulfur. Closed circles show the results of this study. Open squares indicate the results of Ruiz-Garcia *et al* [2] at 392 and 436 K. T_p corresponds to the polymerization temperature (432 K) at ambient pressure. The dashed line represents a least squares fitted line for the present results. The numbers in the figure indicate homologous temperatures (T/T_m).

of the experimental temperatures (T) and melting temperature of the sample (T_m), are almost constant ($T/T_m = 1.03$–1.16) which means that the experimental temperature conditions are parallel to the melting curve (see figure 2). Therefore, viscosity variation with pressure can be comparable to the constant T/T_m condition. The measured viscosity coefficient decreases with increasing pressure, and shows good agreement with the viscosity of polymerized liquid at 436 K and ambient pressure.

In a metallic liquid, viscosity (η_M) increases with decreasing temperature and also with increasing pressure [15]. This behaviour can be interpreted simply as the free volume change in the liquid due to thermal expansion and compaction. η_M at high pressure and temperature conditions can be approximated by the following empirical equation [20]:

$$\eta_M \propto \exp\left(\frac{gT_m}{T}\right) \tag{4}$$

where g is an empirical constant. Equation (4) implies that the viscosity stays constant along the melting curve. However, the present results indicate that the viscosity decreases with pressure at constant homologous temperature. This suggests that the free volume of the liquid does not decrease simply with compaction, and that the structure of the liquid may change continuously

with pressure. The structural similarity between the structure of liquid sulfur at high pressure and the structure of liquid selenium at atmospheric pressure has been reported by Katayama and Tsuji [21]. X-ray diffraction structural analysis of liquid selenium shows that the coordination number and the nearest-neighbour distance of liquid selenium increase with increasing pressure up to 8.4 GPa [22]. This variation corresponds to a gradual structural transition of liquid selenium from twofold-coordinated ordering to fourfold-coordinated ordering [22]. Therefore, if the coordination number of liquid sulfur increases with pressure, longer and weaker bonds must be formed, as observed in liquid selenium, and the viscosity will decrease with pressure. In addition, the polymerization temperature was found to decrease with increasing pressure from the visible absorption technique applied to liquid sulfur [23] and intersect the melting curve at 0.13 GPa [14]. Hence, the effect of the λ-transition on the viscosity, observed at ambient pressure, can be neglected at the present experimental pressures.

According to Brazhkin *et al* [7, 8], a first-order liquid–liquid phase transition (L–L′ transition) occurs in the insulator state of the liquid, as shown in figure 2. Since short range order structures of these liquid phases have not been determined yet, it is uncertain whether the L–L′ transition accompanies large structural changes, which would cause abrupt viscosity change at the phase boundary. Results from the present study show that the viscosity varies smoothly, and no drastic changes are observed up to 9.7 GPa. Therefore, large structural differences between the local structures of two phases (L and L′) are not expected from our viscosity data.

A further phase transition (L′–L″ transition) at higher pressure has also been proposed [7, 8]. This transition corresponds to a non-metallic–metallic liquid transition which is accompanied by a decrease of volume. A dramatic change in liquid structure and physical properties may occur at this boundary.

4. Conclusion

The viscosity of liquid sulfur was measured using the *in situ* x-ray falling sphere method at high pressure and temperature conditions. The measured viscosity ranges over 0.11–0.69 Pa s at 3.2–9.7 GPa and 788–1067 K. The viscosity coefficient decreased continuously with increasing pressure at constant homologous temperature. This implies continuous structural change in the liquid. No evidence for discontinuous structural change was found under the experimental conditions.

Acknowledgments

The authors would like to thank K Sato, T Okada, M Hasegawa and J E Reid for their technical assistance of the experiments. The authors are grateful to M Akaishi for deoxidizing the h-BN capsule. The authors are also grateful to G D Bromiley for helpful comments leading us to improve the manuscript. The authors gratefully acknowledge the comments of two reviewers. The x-ray radiography viscosity measurements were carried out under a contract of the SPring-8 (Proposal number: 2001A0250-ND-np).

References

[1] Bacon R P and Fanelli R J 1943 *J. Am. Chem. Soc.* **65** 639
[2] Ruiz-Garcia J, Anderson E M and Greer S C 1989 *J. Phys. Chem.* **93** 6980
[3] Meyer B 1976 *Chem. Rev.* **76** 367
[4] Biermann C, Winter R, Benmore C and Egelstaff P A 1998 *J. Non-Cryst. Solids* **232–234** 309

[5] Kennedy S J and Wheeler J C 1983 *J. Chem. Phys.* **78** 1523
[6] Wheeler J C, Kennedy S J and Pfeuty P 1980 *Phys. Rev. Lett.* **45** 1748
[7] Brazhkin V V, Voloshin R N, Popova S V and Umnov A G 1991 *Phys. Lett.* A **154** 413
[8] Brazhkin V V, Popova S V and Voloshin R N 1999 *Physica* B **265** 64
[9] Utsumi W, Funakoshi K, Urakawa S, Yamakata M, Tsuji K, Konishi H and Shimomura O 1998 *Rev. High Pressure Sci. Technol.* **7** 1484
[10] Kanzaki M, Kurita K, Fujii T, Kato T, Shimomura O and Akimoto S 1987 *High-Pressure Research in Mineral Physics* ed M H Manghani and Y Shono (Washington, DC: American Geophysical Union) pp 195–200
[11] Urakawa S, Morishima H, Kato T, Suzuki A and Shimomura O 1993 *Photon Fact. Act. Rep.* **G275** 383
[12] Jamieson J C, Fitz J N and Manghani M H 1982 *High-Pressure Research in Geophysics* ed S Akimoto and M H Manghani (Tokyo: Centre for Academic Publishing) pp 27–48
[13] Pease R S 1952 *Acta Crystallogr.* **5** 356
[14] Tonkov E Y 1992 *High Pressure Phase Transformations: a Handbook* (London: Gordon and Breach) pp 647–9
[15] Terasaki H, Kato T, Urakawa S, Funakoshi K, Suzuki A, Okada T, Maeda M, Sato J, Kubo T and Kasai S 2001 *Earth Planet. Sci. Lett.* **190** 93
[16] Faxen H 1925 *Ark. Mat. Astron. Fys.* **19** 1
[17] Kingery W D 1959 *Property Measurements at High Temperatures* (New York: Wiley) p 416
[18] Tsuchiya Y 1994 *J. Phys.: Condens. Matter* **6** 2451
[19] Luo H and Ruoff A L 1993 *Phys. Rev.* B **48** 569
[20] Poirier J P 1988 *Geophys. J.* **92** 99
[21] Katayama Y and Tsuji K 2003 *J. Phys.: Condens. Matter* **15** 6085
[22] Tsuji K 1990 *J. Non-Cryst. Solids* **117/118** 27
[23] Broellos K and Schneider G M 1972 *Ber. Bunsenges. Phys. Chem.* **76** 1106